

Predicting New Heavy Fermion Materials within Carbon-Boron Clathrate Structures

Rishi Rao and Li Zhu*

Department of Physics, Rutgers University, Newark, New Jersey 07102, USA

(Dated: November 21, 2023)

Heavy fermion materials have been a rich playground for strongly correlated physics for decades. However, engineering tunable and synthesizable heavy fermion materials remains a challenge. We strive to integrate heavy fermion properties into carbon boron clathrates as a universal structure which can host a diverse array of interesting physical phenomena. Using a combination of density functional theory and dynamical mean field theory, we study two rare earth carbon boron clathrates, SmB_3C_3 and CeB_3C_3 , and explore properties arising from the strong electronic correlations. We find a significant increase in the density of states at the Fermi level in CeB_3C_3 as the temperature is lowered, indicating the development of a heavy electron state. In SmB_3C_3 , a potential Kondo insulating state is identified. Both findings point to rare earth carbon boron clathrates as novel strongly correlated materials within a universally tunable structure, offering a fresh platform to innovate upon conventional heavy-fermion materials design.

I. INTRODUCTION

Heavy-fermion materials represent a fascinating class of quantum systems with nearly half century of dedicated research [1]. Characterized by extremely large effective electron masses due to strong electron-electron interactions, these materials offer a rich playground for exploring exotic quantum states of matter, including unconventional superconductivity [2–5], quantum criticality [6–8], and non-Fermi liquid behavior [9–12]. While there have been significant advancements in the field of heavy fermions over the decades, persistent challenges and open questions still invite further exploration. Central to this pursuit is deepening our understanding of existing materials and exploring the potential of novel systems. Through the development of new heavy-fermion systems, we can delve deeper into the open questions, advancing both our scientific understanding and opening avenues for technological applications.

The growth in computational capacities and algorithmic sophistication in recent years has accelerated materials science research. However, progress in predicting and discovering new heavy-fermion materials remains incremental [13–20]. Most findings are anchored within a subset of metallic compounds. Conventionally, heavy-fermion materials are exemplified by a limited category of compounds that contain rare-earth ions with partially filled f -shells [21]. These materials exhibit heavy-fermion properties but are limited by a lack of structural diversity, with little structural connection between compounds containing different rare earth ions. Recently, a surge of interest has been directed towards two-dimensional (2D) heavy-fermion materials, offering a new approach to this field. For example, 2D CeIn_3 was produced through artificial superlattices [19], in which electronic properties display striking deviations from the standard low-temperature Fermi liquid behavior. CeSiI was also predicted to be a 2D van der Waals heavy-fermion system

through a data mining theoretical approach [20]. Nevertheless, many of these are derived from the bulk form of pre-existing heavy-fermion compounds. While these materials present a new avenue for exploration, they fail to address the need for greater structural diversity and selective tunability. In addition, it is of interest to create standardized structures where tuning can be applied in a systematic manner while limiting other degrees of freedom. Thus, there is still a pressing need for new material platforms that can be tailored to exhibit either heavy-fermion behavior or other properties of interest in a consistent and adjustable manner.

In this work, we propose a strategy to address these challenges by leveraging the properties of sodalite Carbon-Boron (C-B) clathrates. These unique frameworks, which have been successfully synthesized in the SrB_3C_3 [22] and LaB_3C_3 [23] systems, offer a fresh perspective on the heavy-fermion landscape. The versatility of the clathrate structure allows for targeted doping strategies, and the unique cage-like architecture provides a controlled environment for manipulating electron-electron interactions. The electronic structure of C-B clathrates can be altered immensely by encapsulating guest dopant atoms within the host cavities. For example, Sc-doped C-B clathrate exhibit excellent ferroelectric [24] and piezoelectric properties [25], and doped C-B clathrates have been identified as superconductors with high critical temperatures [26–31]. By selectively introducing rare-earth ions (*e.g.*, lanthanoids) within the cages, the confined space of C-B framework could effectively enhance the interplay between localized f -electrons and itinerant conduction electrons, a key ingredient for heavy-fermion behavior, making C-B clathrates an attractive system in the design of heavy-fermion materials. Furthermore, the successful synthesis of LaB_3C_3 provides a compelling precedent for the viability of other lanthanoids within the C-B clathrate framework.

In this study, guided by state-of-the-art first-principles calculations, we have identified two promising candidates as model systems that have the potential to exhibit heavy-fermion behavior within the clathrate architecture:

* li.zhu@rutgers.edu

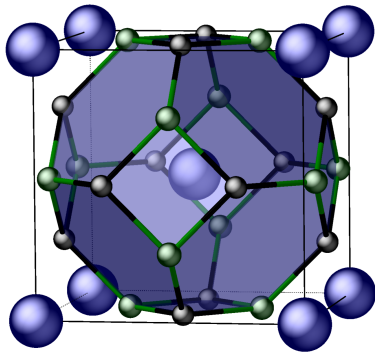


FIG. 1. The crystal structure of the $Pm\bar{3}n$ carbon-boron clathrate. The blue, black, and green spheres represent the Ce/Sm, C, and B atoms, respectively.

CeB_3C_3 and SmB_3C_3 . These two model systems provide a fresh perspective into a strongly correlated landscape within the C-B clathrate platform, laying the foundation for future studies and potentially opening up a new chapter in the study of quantum materials within the clathrate framework.

II. METHODS

The electronic properties were computed through a combination of density functional theory with dynamical mean field theory (DFT+DMFT) as implemented within the COMDMFT software package [32]. The Kohn-Sham DFT equations were solved using a Linear Augmented Plane Wave method as implemented within the Flapwmbpt code [32]. The effective hamiltonian was constructed from Wannier orbitals using the Wannier90 package [33]. Coulomb repulsion and Hund's coupling terms were obtained through the constrained random phase approximation (cRPA) method [34] using the ABINIT software framework [35, 36]. In particular, the values $U = 4.67$ eV and $J = 0.3$ eV were used for $Ce_2B_2C_2$ while $U = 4.95$ eV and $J = 0.4$ eV were used for $Sm_2B_2C_2$. The same values of U and J were used for all temperatures in the DMFT calculations. Slater parametrization is used for generating the Coulomb interaction terms. Continuous time quantum Monte Carlo [37] was used as a solver for the impurity problem and calculations were iterated until charge self-consistency was achieved with double counting being handled through the nominal double counting scheme [38]. All calculations were carried out in the paramagnetic phase with spin-orbit coupling included. Phonon calculations with spin-orbit coupling were carried out using the Phonopy package [39, 40] combined with the Vienna *ab initio* simulation package (VASP) code [41]. See Supplemental Material [42] (see also [34–36, 43–47] therein) for more details on computational methods.

Our first model system centers on the CeB_3C_3

clathrate, which was constructed based on the structure of the recently synthesized SrB_3C_3/LaB_3C_3 . Ce occupies a prominent position in the field of heavy fermion research due to its small $4f$ magnetic moment, which can be easily screened by conduction electrons [48]. This prominence traces back to the discovery of heavy-fermion behavior in $CeAl_3$ [49], and it is responsible for the strongly correlated physics in a wide variety of heavy fermion systems [50–52]. Therefore, incorporating Ce into sodalite C-B clathrate structures is likely to establish a promising foundation for exploring heavy fermion behavior. The absence of imaginary frequencies in the phonon dispersion spectrum of CeB_3C_3 (See supplemental material Fig. S1(a) [42]) suggests structural stability and a negative predicted formation energy (approximately -2.03 eV per formula unit) indicates synthesizability under ambient conditions.

III. RESULTS AND DISCUSSION

We initiate our investigation by examining the ground state electronic structure of CeB_3C_3 , as the Kondo effect stems from the screening of local magnetic moments due to hybridization between conduction and impurity electrons. We find the $2p$ electrons of B and C play a dominant role in this hybridization due to a strong overlap in the density of states near the Fermi level at the LDA level as shown in Fig. 2(a). Anisotropy can also significantly affect the properties and utility of heavy-fermion materials [53]. In order to classify the anisotropy, we examine the contributions from various orbitals to the ground state. Spin-orbit coupling splits the degenerate $4f$ orbital states into $j = 5/2$ and $7/2$ angular momentum components, with the $4f_{5/2}$ being the ground state. The cubic crystal field further removes the degeneracy of the six $4f_{5/2}$ states and splits them into a Γ_8 quartet and a Γ_7 doublet. These states are separated by 14 K, with the lowest energy state being Γ_8 , as is typical for Ce compounds in cubic crystal fields [54]. Since splitting is not significant, its energy scale may match that of the Ruderman–Kittel–Kasuya–Yosida (RKKY) interaction at very low temperatures and enhance formation of long-range magnetic order [55].

Since we are investigating a Kondo lattice system, it is crucial to examine the behavior of the $4f$ electron states near the Fermi level to deduce the onset of coherent scattering and classify the observed properties. In particular, an analysis tracing the evolution of the f -electron density of states from high to low temperatures can show the development of coherence. As shown in Fig. 3(a), the Ce f electrons transition from a local moment phase, exhibiting no spectral weight at the Fermi level, to a delocalized metallic state with a large spectral weight at the Fermi level as the temperature decreases from 200 K to 50 K. At 200 K, the lower and upper Hubbard bands are located around -0.9 eV and 2.5 eV, respectively, with shifts observed when transitioning between local moment

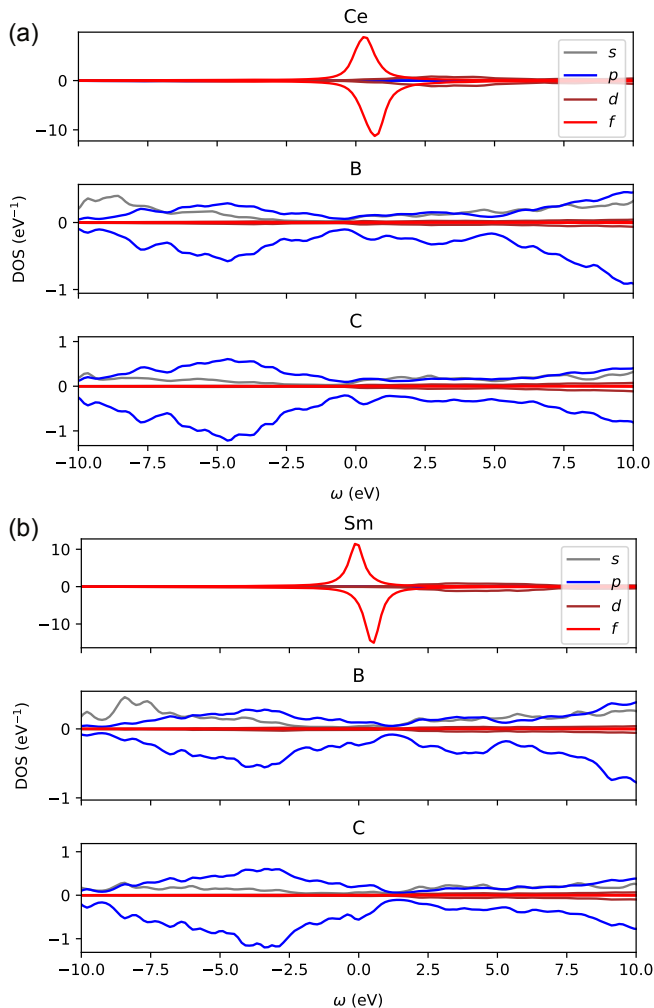


FIG. 2. Projected density of states for (a) CeB_3C_3 and (b) SmB_3C_3 calculated at the DFT level. The Fermi level is set at 0 eV.

and itinerant phases. The concept of Hubbard bands is applicable in this case since dynamical mean field theory maps the Hubbard Model onto a single impurity Anderson model in the limit of infinite dimensions [56]. Therefore, the splitting observed in the Hubbard model, due to on-site electron interactions, is also present in the impurity model treated here.

The spectral weight gradually redistributes away from the lower and upper Hubbard bands as the peak at the Fermi level becomes more resolved. The splitting due to spin-orbit coupling is readily apparent, with the $j = 7/2$ states being elevated above the $j = 5/2$ states by around 276 meV at 50 K. The evolution observed aligns well with the two fluid model [57]. At high temperatures, the lower and upper Hubbard bands, comprised of the $4f$ electron states, contain almost all of the spectral weight. This represents a localization of the Ce electrons and results in the suppression of the Kondo peak. However, as the temperature is lowered, Ce electrons begin to hybridize

with the p electrons of B and C atoms, leading to the formation of itinerant quasiparticles near the Fermi level and a Kondo resonance peak. In Fig. 3(a), we can observe that the spectral weight is rapidly shifted toward the Fermi level when the temperature drops below 100 K, moving closer to the peak of the Fermi level. The low temperature results are qualitatively similar to the model calculations from Bickers *et al.* [58], where a simple effective Hamiltonian is treated using a large-degeneracy expansion and taking into account spin-orbit coupling. At 50 K, a three-peak structure is present with the ground multiplet at -0.4 eV, a Kondo resonance just above the Fermi level, and an excited peak around 0.276 eV. The clear presence of the Kondo resonance peak indicates substantial hybridization between the Ce f electrons and the conduction electrons, suggesting the formation of a heavy fermion state. This resonance indicates a significant admixture of f^0 and f^1 states in the interacting ground state, as expected for coherent scattering off of Ce $4f$ moments.

The observed behavior near the Fermi level lends itself to analysis via Landau-Fermi liquid theory. It is expected that long-lived quasiparticles exist near the Fermi surface, which experience decoherence as the energy scale increases [59, 60]. The lifetime of these quasiparticles is proportional to the inverse of the imaginary part of the self energy on the Matsubara axis, $\tau \propto [\text{Im}\{\Sigma_f(i0^+)\}]^{-1}$, where τ is the quasiparticle lifetime at the Fermi surface and $\Sigma_f(\omega)$ is the local self energy of the f -electron states calculated from DMFT. For CeB_3C_3 between 50 K to 200 K, we predict a convergence towards the Landau-Fermi liquid for the $4f_{5/2}$ states since $\text{Im}\{\Sigma_{5/2}(i0^+)\}$ rapidly approaches zero as temperature is lowered to 50 K as shown in Fig. 4(a). This indicates a fermi-liquid energy scale of around $T^* \approx 50\text{K}$. The $4f_{7/2}$ states remain coherent throughout the temperature evolution but contain no weight at the Fermi level. This convergence towards coherence provides evidence for the formation of a Fermi-liquid state at low temperatures. The spectral function at 50 K provides interesting insights into the strong electronic correlations. We observe an almost directional dependence on the Fermi surface, as indicated by the lack of spectral weight at the R point. Additionally, we find that electron hole pockets emerge at the M points in the cubic Brillouin zone.

Heavy fermion materials are typically characterized by a substantial linear temperature dependence of specific heat characterized by the Sommerfeld coefficient γ at low temperatures [61]. To estimate this quantity, we use the renormalized density of states. At 50 K, the quasiparticle renormalization for the f states is estimated by [60]

$$Z = \left[1 - \frac{d\text{Im}\{\Sigma_{f,5/2}(i\omega_n)\}}{d(i\omega_n)} \Big|_{i\omega_n \rightarrow 0^+} \right]^{-1}, \quad (1)$$

which yields a value of $Z_{50\text{K},f} = 0.158$. The linear part

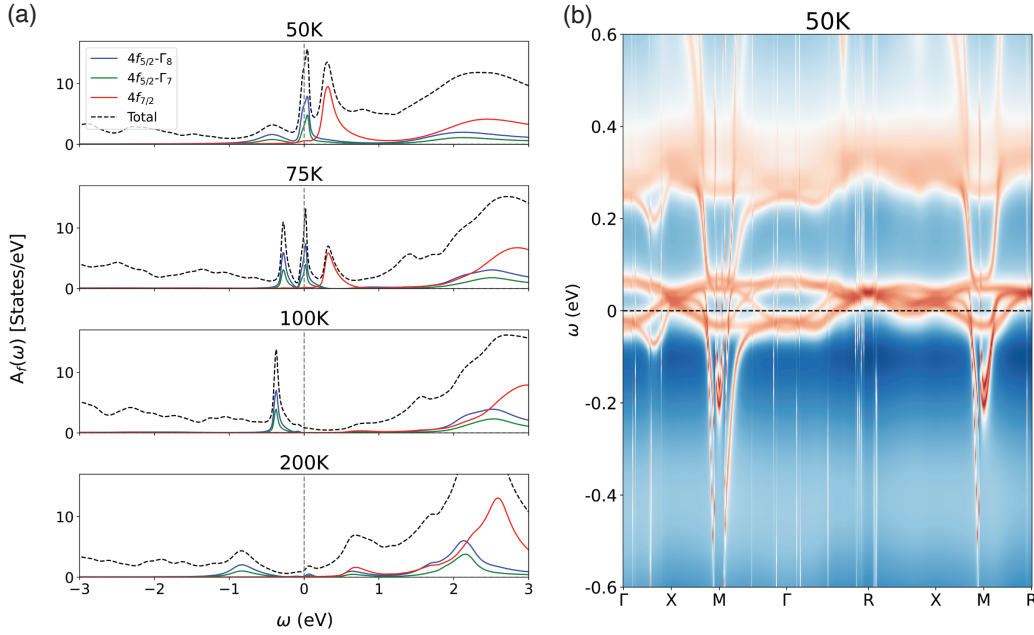


FIG. 3. Temperature evolution of Ce 4*f*-electron density of states and spectral function at 50K. (a) Temperature evolution of the 4*f*-electron density of states of CeB₃C₃. (b) Spectral function $A(\vec{k}, \omega)$ of CeB₃C₃ at $T = 50$ K.

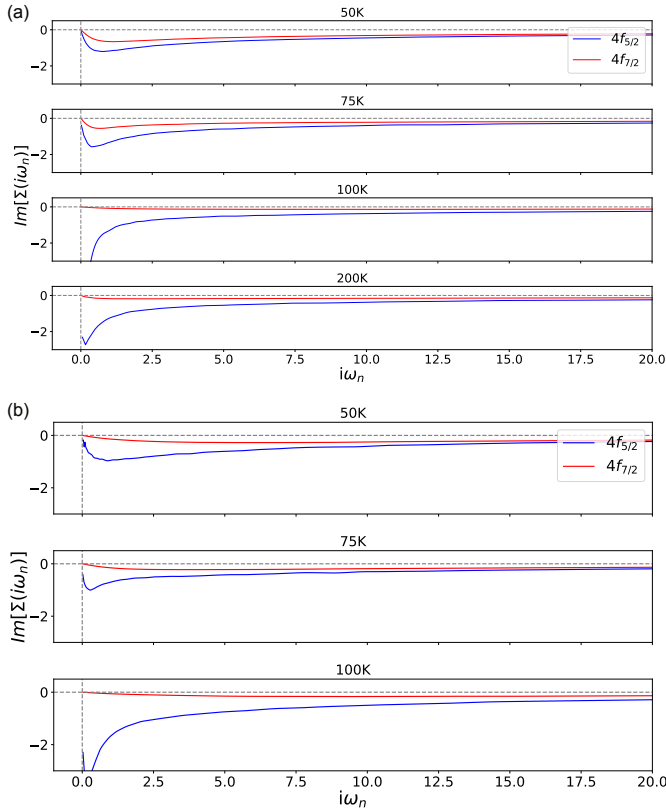


FIG. 4. Temperature evolution of imaginary part of the 4*f* electron self energy for each angular momentum state on the Matsubara axis for (a) CeB₃C₃ and (b) SmB₃C₃.

of the specific heat, γ , can subsequently be estimated as

$$\gamma = \frac{\pi^2 k_B^2}{3} \frac{N^{LDA}(E_f)}{Z_{50K,f}}, \quad (2)$$

where $N^{LDA}(E_f) = 12.342 \text{ eV}^{-1}$ is the density of states at the Fermi level, estimated from the local density approximation (LDA) DFT calculations, and k_B is Boltzmann's constant. We use the density of states from LDA since the temperature of 50 K in DMFT simulations is not low enough to fully capture the transition to a heavy fermion state. Incorporating these values, we predict a linear specific heat coefficient of $\gamma = 183 \frac{mJ}{molK^2}$ which is an order of magnitude above simple metals and in line with concentrated Kondo systems [62].

Sm-based compounds offer another avenue to engineer strong correlations into C-B clathrates. In general, Sm compounds exhibit mysterious properties even within the sphere of strongly correlated materials. Theoretical explanations for small moment magnetism, mixed valency [63], and topological Kondo insulating effects [64] remain elusive for this category of compounds. Due to the tendency for valence fluctuations and strongly anisotropic magnetic moments [65, 66], a clathrate compound containing Sm could unveil new and captivating physics, potentially leading to novel applications. Furthermore, such unique structures may shed light on open questions regarding the role of Sm in strongly correlated materials by providing a new crystal environment. Computed phonon dispersion spectra of SmB₃C₃ (See supplemental material Fig. S1 (b) [42]) show no imaginary phonon frequencies, indicating structural stability. Additionally, a

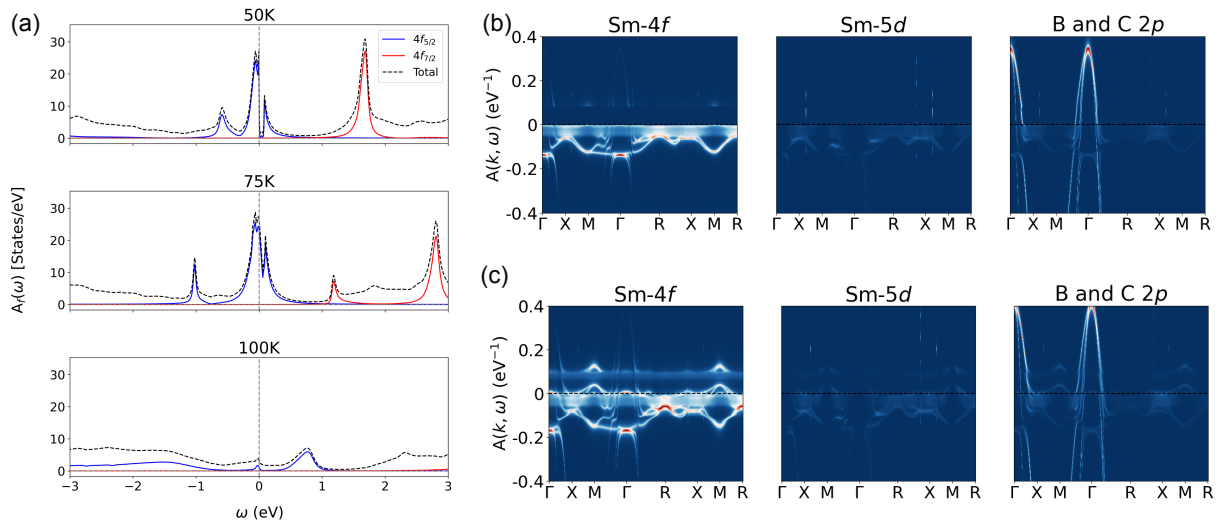


FIG. 5. (a) Temperature dependent evolution of the f -electron density of states of SmB_3C_3 . Orbital-resolved spectral function for SmB_3C_3 at (a) 50K and (b) 75K. Dominant hybridization occurs from B and C $2p$ orbitals. The y -axis units are in eV , and intensity is scaled for clarity.

negative formation energy at atmospheric pressure (approximately -0.98 eV per formula unit) is promising for future synthesis efforts.

To classify the strong electronic correlations, we first investigate the ground state electronic structure of SmB_3C_3 . At higher temperatures, localized f -moment electrons generally disperse within the lower and upper Hubbard bands. Figure 5(a) depicts the transition of the f -electron DOS from 100 K to 50 K, where a clear transference of spectral weight towards the Fermi surface is evident, indicating strong Kondo lattice effects. The spectral weight from the wide peaks situated at around -1.5 eV and 0.75 eV steadily transfer towards the Fermi level and sharpens, resulting in localized peaks in the density of states. This suggests that the local moment phase is screened as the temperature decreases. The f -level occupancy is $n_f = 5.59$ at $T = 50$ K, in contrast to $n_f = 5.12$ at $T = 100$ K, implying that SmB_3C_3 enters a mixed valency regime as the temperature drops. The zero frequency imaginary part of the self energy for the $4f_{5/2}$ states never reaches zero as shown in Fig. 4(b). In addition, the occupancy of the $4f_{5/2}$ state is quite large indicating a gapped phase.

The orbital-resolved spectral functions (Fig. 5(b-c)) indicate that the predominant hybridization contributions in SmB_3C_3 originates from the B and C p orbitals. As the temperature decreases from 75 K to 50 K, a discernible enhancement in orbital weight near the Fermi level becomes evident for the p orbitals. Concurrently, a strong renormalization of spectral weight occurs below the Fermi level in the Sm f orbitals. The formation of a gap is apparent, similar to the Kondo insulating gap found in black phase of SmS [67]. The emerging state, primarily dictated by the $j = 5/2$ angular momentum states, exhibits a 90 meV gap at 50 K. This supports the

hypothesis that SmB_3C_3 may be a Kondo insulator.

IV. CONCLUSION

In summary, both clathrates display signs of strong Kondo lattice behavior as temperature is lowered. They are predicted to be dynamically stable and thermodynamically favorable under ambient pressure, making them strong candidates for experimental synthesis. CeB_3C_3 is predicted to be a potential heavy fermion compound with a Kondo temperature below 50 K. This clathrate displays both Fermi-liquid behavior and concentrated Kondo lattice behavior at intermediate temperatures. SmB_3C_3 appears to transition towards a Kondo insulating state, with a notable redistribution of spectral weight around the Fermi level coupled with a very small band gap. Though the orbital-resolved spectral functions do not unveil topological characteristics at 50 K and ambient pressure, applying pressure may reveal novel aspects of the phase diagram. These observations suggest an intriguing potential for future research. Moreover, the discovery of the two heavy-fermion clathrates ushers in a new domain of materials that exhibit strong electronic correlation effects, providing a robust platform for investigating such phenomena.

ACKNOWLEDGMENTS

This work was supported by the startup funds of the office of the Dean of SASN of Rutgers University-Newark. The authors acknowledge the Office of Advanced Research Computing (OARC) at Rutgers for providing ac-

cess to the Amarel cluster and associated research computing resources.

-
- [1] S. Wirth and F. Steglich, Exploring heavy fermions from macroscopic to microscopic length scales, *Nat. Rev. Mats.* **1**, 16051 (2016).
- [2] B. White, J. Thompson, and M. Maple, Unconventional superconductivity in heavy-fermion compounds, *Phys. C: Supercond.* **514**, 246 (2015).
- [3] M. R. Norman, The challenge of unconventional superconductivity, *Science* **332**, 196 (2011).
- [4] M. Smidman, O. Stockert, J. Arndt, G. M. Pang, L. Jiao, H. Q. Yuan, H. A. Vieyra, S. Kitagawa, K. Ishida, K. Fujiwara, *et al.*, Interplay between unconventional superconductivity and heavy-fermion quantum criticality: CeCu₂Si₂ versus YbRh₂Si₂, *Philos. Mag.* **98**, 2930 (2018).
- [5] N. D. Mathur, F. M. Grosche, S. R. Julian, I. R. Walker, D. M. Freye, R. K. W. Haselwimmer, and G. G. Lonzarich, Magnetically mediated superconductivity in heavy fermion compounds, *Nature* **394**, 39 (1998).
- [6] P. Gegenwart, Q. Si, and F. Steglich, Quantum criticality in heavy-fermion metals, *Nat. Phys.* **4**, 186 (2008).
- [7] O. Stockert and F. Steglich, Unconventional quantum criticality in heavy-fermion compounds, *Annu. Rev. Condens. Matter Phys.* **2**, 79 (2011).
- [8] P. Aynajian, E. H. da Silva Neto, A. Gyenis, R. E. Baumbach, J. D. Thompson, Z. Fisk, E. D. Bauer, and A. Yazdani, Visualizing heavy fermions emerging in a quantum critical kondo lattice, *Nature* **486**, 201 (2012).
- [9] P. Coleman, Theories of non-fermi liquid behavior in heavy fermions, *Phys. B: Condens.* **259-261**, 353 (1999).
- [10] S. Seiro, L. Jiao, S. Kirchner, S. Hartmann, S. Friedemann, C. Krellner, C. Geibel, Q. Si, F. Steglich, and S. Wirth, Evolution of the kondo lattice and non-fermi liquid excitations in a heavy-fermion metal, *Nat. Commun.* **9**, 3324 (2018).
- [11] H. v. Löhneysen, T. Pietrus, G. Portisch, H. G. Schlager, A. Schröder, M. Sieck, and T. Trappmann, Non-fermi-liquid behavior in a heavy-fermion alloy at a magnetic instability, *Phys. Rev. Lett.* **72**, 3262 (1994).
- [12] H. v. Löhneysen, Non-fermi-liquid behavior in heavy-fermion systems, *Phys. B: Condens.* **206-207**, 101 (1995).
- [13] J. D. Thompson and Z. Fisk, Progress in heavy-fermion superconductivity: Ce115 and related materials, *J. Phys. Soc. Jpn.* **81**, 011002 (2012).
- [14] M. Naritsuka, T. Terashima, and Y. Matsuda, Controlling unconventional superconductivity in artificially engineered f-electron kondo superlattices, *J. Condens. Matter Phys.* **33**, 273001 (2021).
- [15] G. R. Stewart, Z. Fisk, J. L. Smith, J. O. Willis, and M. S. Wire, New heavy-fermion system, npbe₁₃, with a comparison to ube₁₃ and pube₁₃, *Phys. Rev. B* **30**, 1249 (1984).
- [16] E. Svanidze, A. Amon, R. Borth, Y. Prots, M. Schmidt, M. Nicklas, A. Leithe-Jasper, and Yu. Grin, Empirical way for finding new uranium-based heavy-fermion materials, *Phys. Rev. B* **99**, 220403 (2019).
- [17] J. Tang and K. A. Gschneidner, Searching for new heavy fermion materials in cerium intermetallic compounds, *J. Less-Common. Met.* **149**, 341 (1989).
- [18] Z. Fisk, Searching for heavy fermion materials, *Phys. B: Condens. Matter* **378-380**, 13 (2006).
- [19] H. Shishido, T. Shibauchi, K. Yasu, T. Kato, H. Kontani, T. Terashima, and Y. Matsuda, Tuning the Dimensionality of the Heavy Fermion Compound CeIn₃, *Science* **327**, 980 (2010).
- [20] B. G. Jang, C. Lee, J.-X. Zhu, and J. H. Shim, Exploring two-dimensional van der waals heavy-fermion material: Data mining theoretical approach, *npj 2D Mater. Appl.* **6**, 80 (2022).
- [21] P. Coleman, Heavy fermions and the kondo lattice: a 21st century perspective (2015), arXiv:1509.05769 [cond-mat.str-el].
- [22] L. Zhu, G. M. Borstad, H. Liu, P. A. Guñka, M. Guerette, J.-A. Dolyniuk, Y. Meng, E. Greenberg, V. B. Prakapenka, B. L. Chaloux, A. Epshteyn, R. E. Cohen, and T. A. Strobel, Carbon-boron clathrates as a new class of *sp*³-bonded framework materials, *Sci. Adv.* **6**, eaay8361 (2020).
- [23] T. A. Strobel, L. Zhu, P. A. Guñka, G. M. Borstad, and M. Guerette, A lanthanum-filled carbon-boron clathrate, *Angew. Chem. Int. Ed.* **60**, 2877 (2021).
- [24] L. Zhu, T. A. Strobel, and R. E. Cohen, Prediction of an Extended Ferroelectric Clathrate, *Phys. Rev. Lett.* **125**, 127601 (2020).
- [25] Z. Tan, H. Zhang, X. Wu, J. Xing, Q. Zhang, and J. Zhu, New high-performance piezoelectric: Ferroelectric carbon-boron clathrate, *Phys. Rev. Lett.* **130**, 246802 (2023).
- [26] N. Geng, K. P. Hilleke, L. Zhu, X. Wang, T. A. Strobel, and E. Zurek, Conventional High-Temperature Superconductivity in Metallic, Covalently Bonded, Binary-Guest C-B Clathrates, *J. Am. Chem. Soc.* **145**, 1696 (2023), PMID: 36622785.
- [27] L. Zhu, H. Liu, M. Somayazulu, Y. Meng, P. A. Guñka, T. B. Shiehl, C. Kenney-Benson, S. Chariton, V. B. Prakapenka, H. Yoon, J. A. Horn, J. Paglione, R. Hoffmann, R. E. Cohen, and T. A. Strobel, Superconductivity in SrB₃C₃ clathrate, *Phys. Rev. Res.* **5**, 013012 (2023).
- [28] T.-T. Gai, P.-J. Guo, H.-C. Yang, Y. Gao, M. Gao, and Z.-Y. Lu, Van hove singularity induced phonon-mediated superconductivity above 77 k in hole-doped srb₃c₃, *Phys. Rev. B* **105**, 224514 (2022).
- [29] P. Zhang, X. Li, X. Yang, H. Wang, Y. Yao, and H. Liu, Path to high-*T*_c superconductivity via rb substitution of guest metal atoms in the Sr₃C₃ clathrate, *Phys. Rev. B* **105**, 094503 (2022).
- [30] S. Di Cataldo, S. Qulaghasi, G. B. Bachelet, and L. Boeri, High-*T*_c superconductivity in doped boron-carbon clathrates, *Phys. Rev. B* **105**, 064516 (2022).
- [31] J.-N. Wang, X.-W. Yan, and M. Gao, High-temperature superconductivity in srb₃c₃ and bab₃c₃ predicted from first-principles anisotropic migdal-eliashberg theory, *Phys. Rev. B* **103**, 144515 (2021).
- [32] A. Kutepov, V. Oudovenko, and G. Kotliar, Linearized self-consistent quasiparticle GW method: Application to semiconductors and simple metals, *Comput. Phys. Commun.* **219**, 407 (2017).

- [33] A. A. Mostofi, J. R. Yates, Y.-S. Lee, I. Souza, D. Vanderbilt, and N. Marzari, wannier90: A tool for obtaining maximally-localised wannier functions, *Comput. Phys. Commun.* **178**, 685 (2008).
- [34] B. Amadon, T. Applencourt, and F. Bruneval, Screened coulomb interaction calculations: Crpa implementation and applications to dynamical screening and self-consistency in uranium dioxide and cerium, *Phys. Rev. B* **89**, 125110 (2014).
- [35] X. Gonze, B. Amadon, G. Antonius, F. Arnardi, L. Baguet, J.-M. Beuken, J. Bieder, F. Bottin, J. Bouchet, E. Bousquet, N. Brouwer, F. Bruneval, G. Brunin, T. Cavignac, J.-B. Charraud, and Others, The abinit project: Impact, environment and recent developments, *Comput. Phys. Commun.* **248**, 107042 (2020).
- [36] A. H. Romero, D. C. Allan, B. Amadon, G. Antonius, T. Applencourt, L. Baguet, J. Bieder, F. Bottin, J. Bouchet, E. Bousquet, F. Bruneval, G. Brunin, D. Caliste, M. Côté, J. Denier, and Others, Abinit: Overview, and focus on selected capabilities, *J. Chem. Phys.* **152**, 124102 (2020).
- [37] E. Gull, A. J. Millis, A. I. Lichtenstein, A. N. Rubtsov, M. Troyer, and P. Werner, Continuous-time monte carlo methods for quantum impurity models, *Rev. Mod. Phys.* **83**, 349 (2011).
- [38] K. Haule, C.-H. Yee, and K. Kim, Dynamical mean-field theory within the full-potential methods: Electronic structure of CeIrIn₅, CeCoIn₅, and CeRhIn₅, *Phys. Rev. B* **81**, 195107 (2010).
- [39] A. Togo and I. Tanaka, First principles phonon calculations in materials science, *Scr. Mater.* **108**, 1 (2015).
- [40] A. Togo, First-principles phonon calculations with phonopy and phono3py, *J. Phys. Soc. Jpn.* **92**, 012001 (2023).
- [41] G. Kresse and J. Furthmüller, Efficient iterative schemes for ab initio total-energy calculations using a plane-wave basis set, *Phys. Rev. B* **54**, 11169 (1996).
- [42] See Supplemental Material at <http://link.aps.org/supplemental/x>, which includes details on the DMFT calculations, phonon spectra, LDA density of states, and LDA bandstructure, .
- [43] M. Torrent, F. Jollet, F. Bottin, G. Zérah, and X. Gonze, Implementation of the projector augmented-wave method in the ABINIT code: Application to the study of iron under pressure, *Comput. Mater. Sci.* **42**, 337 (2008).
- [44] A. V. Nikolaev and A. V. Tsvyashchenko, The puzzle of the $\gamma \rightarrow \alpha$ and other phase transitions in cerium, *Phys.-Usp.* **55**, 657 (2012).
- [45] F. H. Ellinger and W. H. Zachariasen, The crystal structure of samarium metal and of samarium monoxide¹, *J. Am. Chem. Soc.* **75**, 5650 (1953).
- [46] A. R. Oganov, J. Chen, C. Gatti, Y. Ma, Y. Ma, C. W. Glass, Z. Liu, T. Yu, O. O. Kurakevych, and V. L. Solozhenko, Ionic high-pressure form of elemental boron, *Nature* **457**, 863 (2009).
- [47] R. B. Lindsay, The carbon atom model and the structure of diamond, *Phys. Rev.* **29**, 497 (1927).
- [48] A. Galler, S. Ener, F. Maccari, I. Dirba, K. P. Skokov, O. Gutfleisch, S. Biermann, and L. V. Pourovskii, Intrinsically weak magnetic anisotropy of cerium in potential hard-magnetic intermetallics, *npj Quantum Mater.* **6**, 2 (2021).
- [49] K. Andres, J. E. Graebner, and H. R. Ott, *4f*-Virtual-Bound-State Formation in CeAl₃ at Low Temperatures, *Phys. Rev. Lett.* **35**, 1779 (1975).
- [50] J. Flouquet, P. Haen, P. Lejay, P. Morin, D. Jaccard, J. Schweizer, C. Vettier, R. Fisher, and N. Phillips, Magnetic instability in Ce heavy fermion compounds, *J. Magn. Magn. Mater.* **90-91**, 377 (1990).
- [51] M. Matsumoto, M. J. Han, J. Otsuki, and S. Y. Savrasov, Magnetic quantum critical point and dimensionality trend in cerium-based heavy-fermion compounds, *Phys. Rev. B* **82**, 180515 (2010).
- [52] W. Zhou, C. Q. Xu, B. Li, R. Sankar, F. M. Zhang, B. Qian, C. Cao, J. H. Dai, J. Lu, W. X. Jiang, D. Qian, and X. Xu, Kondo behavior and metamagnetic phase transition in the heavy-fermion compound CeBi₂, *Phys. Rev. B* **97**, 195120 (2018).
- [53] P. J. W. Moll, T. Helm, S.-S. Zhang, C. D. Batista, N. Harrison, R. D. McDonald, L. E. Winter, B. J. Ramshaw, M. K. Chan, F. F. Balakirev, B. Batlogg, E. D. Bauer, and F. Ronning, Emergent magnetic anisotropy in the cubic heavy-fermion metal CeIn₃, *npj Quantum Mater.* **2**, 46 (2017).
- [54] S. Souma, H. Kumigashira, T. Ito, T. Sato, T. Takahashi, and S. Kunii, Crystal-field splitting in CeB₆ observed by ultrahigh-resolution photoemission spectroscopy, *J. Electron Spectrosc. Relat. Phenom.* **114-116**, 729 (2001).
- [55] A. M. Konic, Y. Zhu, A. J. Breindel, Y. Deng, C. M. Moir, M. B. Maple, C. C. Almasan, and M. Dzero, Vanishing RKKY interactions in Ce-based cage compounds, *J. Phys. Condens. Matter* **35**, 465601 (2023).
- [56] A. Georges and G. Kotliar, Hubbard model in infinite dimensions, *Phys. Rev. B* **45**, 6479 (1992).
- [57] Y. feng Yang, Two-fluid model for heavy electron physics, *Rep. Prog. Phys.* **79**, 074501 (2016).
- [58] N. E. Bickers, D. L. Cox, and J. W. Wilkins, Self-consistent large-*n* expansion for normal-state properties of dilute magnetic alloys, *Phys. Rev. B* **36**, 2036 (1987).
- [59] Chapter 4 fermi-liquid, heavy fermi-liquid, and non-fermi-liquid models, in *Heavy-Fermion Systems*, Handbook of Metal Physics, Vol. 2, edited by P. Misra (Elsevier, 2008) pp. 51–86.
- [60] P. Coleman, *Introduction to Many-Body Physics* (Cambridge University Press, 2015).
- [61] H. Löhneysen, Strongly correlated electron systems, in *Encyclopedia of Condensed Matter Physics*, edited by F. Bassani, G. L. Liedl, and P. Wyder (Elsevier, Oxford, 2005) pp. 46–54.
- [62] C. D. Bredl, F. Steglich, and K. D. Schotte, Specific heat of concentrated kondo systems: (La, Ce)Al₂ and CeAl₂, *Z. Phys. B.* **29**, 327 (1978).
- [63] R. Shiina, Theory of field-insensitive heavy fermion in Sm compounds, *AIP Adv.* **8**, 101301 (2018).
- [64] M. Neupane, N. Alidoust, S.-Y. Xu, T. Kondo, Y. Ishida, D. J. Kim, C. Liu, I. Belopolski, Y. J. Jo, T.-R. Chang, H.-T. Jeng, T. Durakiewicz, L. Balicas, H. Lin, A. Bansil, *et al.*, Surface electronic structure of the topological kondo-insulator candidate correlated electron system SmB₆, *Nat. Commun.* **4**, 2991 (2013).
- [65] S. D. Mahanti, T. A. Kaplan, and M. Barma, Valence fluctuation in samarium compounds—A theoretical approach, *J. Appl. Phys.* **49**, 2084 (2008).
- [66] K. A. McEwen, P. F. Touborg, G. J. Cock, and L. W. Roeland, Magnetic properties of samarium, *J. Phys. F.* **4**, 2264 (1974).

- [67] C.-J. Kang, H. C. Choi, K. Kim, and B. I. Min, Topological properties and the dynamical crossover from mixed-valence to kondo-lattice behavior in the golden phase of SmS , *Phys. Rev. Lett.* **114**, 166404 (2015).